Adsorption Investigations on the Removal of Azoic Dye by Untreated Wood Sawdust

Abstract

Batch adsorption of the azoic dye Congo red (CR) was carried out successfully on untreated low-cost wood sawdust. The impact of several variables (contact time, amount of solid adsorbent, initial adsorbate concentration, temperature, and pH) on the sorption process was studied. A maximum removal efficiency was achieved after 50 minutes at pH = 5 and 25 °C. To characterize the adsorbent, FTIR, SEM, EDX, and BET analyses were performed. The equilibrium isotherms were described using four alternative models. The data were found to fit the Freundlich model the best. The kinetic analysis demonstrates that the process is best represented by a pseudo-second-order model. The thermodynamic studies revealed the spontaneity and the exothermic nature of the sorption process. The optimal isotherm model served as the foundation for the design of a one-stage batch adsorber for the sorption of CR onto wood sawdust.

Keywords: Congo red, sawdust, adsorbent, adsorption.

1. Introduction

Toxic heavy metals **[1]**, textile dyes **[2,3]**, pesticides, and organic pollutants **[**4,5] have all been detected in surface and ground water. These contaminants negatively affect both environment and humans. Azo dyes are the most commonly used dyes, accounting for more than 60% of all dyes; they are commonly applied in the pharmaceutical, textile, printing, and paper manufacture.Azo dyes may contain one or more chromophore attached to the aromatic rings. (see Figure 1). Azo dyes are particularly stable to light and harsh conditions due to the presence of the azo groups and the resonance structure, which makes them perfect for chemical industries. Congo red dye is an important example for azoic dyes and it is also considered a good model for high molecular weight compounds with complex structure**[6].**

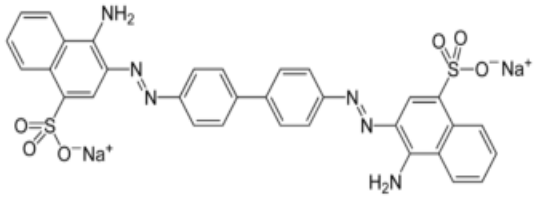

Figure 1: Chemical structure of the azoic dye Congo red

Due to the amino groups connected to the aromatic ring, Congo Red (diazo dye) is regarded as carcinogenic. The occurrence of aromatic structures makes azo dyes resistant to natural deterioration. As a result, treatment of Congo Red dye-contaminated water is a necessity **[7]**.A variety of techniques, including adsorption **[7-9]**, coagulation–flocculation **[10]**, ion exchange **[11]**, and photocatalysis **[12]**, have been suggested to eliminate Congo Red from contaminated water. Among of all the mentioned methods, Due to its benefits of cheap cost, abundant supply of adsorbents, large adsorption capacity, simple restoration possibility, and minimal energy demand., adsorption will continue to be of significant importance. The kind and characteristics of the adsorbent have an impact on the adsorption process. various researches showed the possibility of using lignocellulosic materials such as rice straw, bagasse and wood sawdust as biosorbentsto remove water pollutants **[13,14]**.

Sawdust (from softwood or hardwood) is a solid waste of carpentry workshops. It is available in Egypt at large amounts and low prices. Wood sawdust is a lignocellulosic material that contains cellulose, hemicelluloses, lignin, and minor amounts of extraneous materials. Due to its chemical structure, it has a potential as an alternative adsorbent for industrial wastewater polluted with CR dye.

The current study aims to investigate the efficacy of unmodified wood sawdust as an ecofriendly solid desiccant for batch removal of Congo red dye.

2. Materials and methods

2.1 Solid desiccant preparation

Wood sawdust (SD) was providedby a local carpentry workshop in Damietta city, Egypt. It was washed multiple times with water from the tap and then with distilled water to eliminate dirt and surface contaminants. It was then left to dry in a furnace (PS.3A, Advanced Technology, UK), which provides uniform temperatures throughout (60-70°C) for 2 hours. A batch with a particle size ranging from 2 mm to 75 mm was chosen after the dry material was sieved using a SAMA Sieve Shaker.

2.2. Congo red dye solution preparation

A Stock solution of Congo red dye (500 mg/l) was created by dissolving 0.5g of the solid dye in 1litre of distilled water. The stock solution was diluted to acquire different dye concentrations.

2.3 Characterization of SD adsorbent

SEM imaging was used to compare the surface morphological properties of the solid adsorbent prior to and aftersorption experiments(SEM, JEOL-JSM-6510LV, Akishima, Japan). The infrared (IR) spectra were recorded in the range from 4000 to 400 cm^{-1} region using a JASCOFTIR-4100 spectrophotometer prior to and after the adsorption. Based on the BET equation, the Brunauer-Emmett-Tellersurface area (SBET) was calculated. Oxford instruments, Oxford, UK. Inca Penta FET x3 electron diffraction spectrum [EDS], were used to perform quantitative elemental studies on the adsorbent. A ZetasizerNano-ZS-90 [Malvern Instruments, Malvern, UK] was used to measure the zeta potential of wood sawdust.

2.4 Batch Adsorption Investigations

Using the batch technique, it was determined how the experiment's parameters (contact time, dose of adsorbent, temperature, pH, and starting adsorbate concentration) affect the adsorption process. The experiments in this work were conducted using simulated wastewater that has been CR-contaminated. Duringall Adsorption experiments the adsorbent- adsorbate mixtures were kept in a temperature controlled shaker water bath (Wisd laboratory instruments, DAHAN Scientific co., ltd, 30, Korea) at 240 rpm. The dye solution's pH was modified by using a solution of 0.1 N HCl and 0.1 N NaOH and the pH values were monitoredusing a pH–meter (Hanna- Instruments 8519, pH 211, Canada).The adsorbent's capacity was calculated using the formula below:

$$q_t = \frac{(C_o - C_t)V}{W} \qquad (1)$$

Using the following equation, the percentage of CR removed was determined:

$$\%R = \frac{C_o - C_t}{C_o} \times 100 \qquad (2)$$

where q_t(mg/g) denotes the quantity of Congo red dye adsorbed on wood sawdust at time t, C_o(mg/l) and C_t(mg/l) are the Congo red dye initial strength and at time t, respectively. The starting volume of the dye solution is given by V(l), and the utilized adsorbent's amount is given by W(g) **[15]**.

2.5 Studies on equilibrium and adsorption isotherms

The experimental results were fitted to four equilibrium models to conduct the isotherm investigation (Langmuir, Freundlich, Timken, and Dubinin-Radushkevich model).
The Langmuir isotherm presupposes homogenous sites and monolayer distribution for adsorption. The linear Langmuir form is:

$$\frac{c_e}{q_e} = \frac{1}{q_m k_l} + \frac{c_e}{q_m} \qquad (3)$$

where: q_m is the maximal adsorption capacity (mg/g), and k_l is the Langmuir affinity constant (l/ mg)associated withq_m and adsorption velocity.
The adsorption on heterogeneous surfaces is what the Freundlich model believes to occur on. Given as follows is the linear Freundlich form:

$$\ln q_e = \frac{1}{n} \ln c_e + \ln k_f \qquad (4)$$

where: k_f is the Freundlich constant which is related to the adsorption capacity (mg/g) and 1/n denotes the adsorption process's favorability. Adsorption is advantageous if 1/n values fall between 0 and 1.
Temkin's approach assumes that a homogeneous distribution of binding energy characterize adsorption and that the heat of molecules adsorption declines linearly with coverage. The linear Temkin form is given as:

$$q_e = q_m \ln k_t + q_m \ln c_e \qquad (5)$$

Where:q_m and k_t are the Temkin constants related to adsorption capacity in (l /mg) and the heat of adsorption (J/mole)**[16]**.
According to the Dubinin-Radushkevich model, adsorption occurs on heterogeneous surfaces with high solute activity, a wide range of concentrations, and a Gaussian energy distribution. The Dubinin–Radushkevich linear form is given as:

$$\ln q_e = \ln q_m - D\varepsilon^2 \qquad (6)$$

$$\varepsilon = RT \ln \frac{c_e + 1}{c_e} \qquad (7)$$

Where: ε is Polanyi potential, R is gas constant (kJ /mol K), T is the temperature in (K), and D, qm are Dubinin constants.

2.6 Kinetic studies

Two kinetic models were employed to depict the adsorption mechanism and the rate limiting step. The pseudo-first-order rate equation is given as:

$$\log(q_e - q_t) = \log q_e - \frac{k_1 t}{2.303} \qquad (8)$$

Where: q_t is the adsorption capacity at any time (mg/g), and k_1 is the first-order rate constant.
The pseudo-second-order rate equation is given as:

$$\frac{t}{q_t} = \frac{1}{k_2 {q_e}^2} + \frac{t}{q_e} \qquad (9)$$

Where: k_2 is the rate constant of the pseudo-second-order adsorption**[17]**.

2.7 Thermodynamic studies

The goal of thermodynamic analysis is to ascertain thermodynamic parameters like Gibbs free energy (ΔG, kJ /mol), enthalpy (ΔH, kJ /mol), and entropy (ΔS, kJ /mol. K). These parameters are used to determine the adsorption process's spontaneity. They are computed using the Van't Hoff equation, as follows:

$$\Delta G = -RT \ln K \qquad (10)$$

$$\ln K = \frac{\Delta S}{R} - \frac{\Delta H}{RT} \qquad (11)$$

$$K = \frac{q_e}{c_e} \qquad (12)$$

Where: R is the gas constant (8.314 J /mol. K) and T is the temperature in kelvin.

3. Results and discussion

3.1 Characterization of unmodified SD.

3.1.1. Scanning Electron Microscopy (SEM)

SEM micrographs of the SD desiccant before dye adsorption revealed an irregular texture, rough surface, and varying porosity levels, all of which provide suitable sites for dye molecule adsorption (Figure 2(a)) and making SD a suitable adsorbent**[18,19]**.

After dye adsorption, a significant area of SD is coated with dye molecules in the shape of flakes, hence the SEM image of SD after adsorption exhibited smooth surface because of the trapping of dye molecules on its surface, as can be seen in Figure 2 (b).

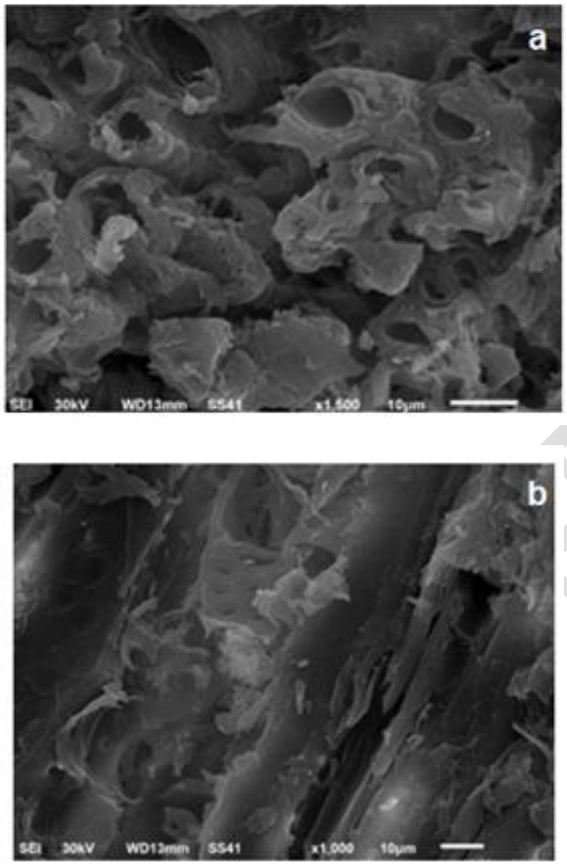

Figure 2:SEM micrograph of wood saw dust (a) before CR adsorption, (b) after CR adsorption.

3.1.2. Fourier Transform Infra-red (FT-IR) spectra

As shown in Figure 3(a), the unmodified wood sawdust FTIR spectrum shows a broad peak at 3439 cm^{-1} which may be attributed to the alcoholic and/or the phenolic OH stretching and the intermolecular hydrogen bonding. The absorption band of alkyl group appears at 2924 cm^{-1}. The peak at 1740 cm^{-1} is assigned to the existenceof carbonyl group of the aliphatic ester of lignin and/or hemicellulose, while the absorption band at 1602 cm^{-1} may be assigned to the existence of conjugated C=C of the aromatic nucleus **[18]**. The bands at 1378 cm^{-1} and 1256 cm^{-1} are due to the CH_2 external deformation. An absorption band at 1113 cm^{-1} is caused by C-O-C of the glycoside ether. The ether groups of lignin, cellulose, and hemicellulose are allocated to the C-O or C-O-C stretching band at 1029 cm^{-1}**[20,21].** Figure 3(b) shows the FTIR spectrum of dye saturated wood sawdust.A characteristic band of Congo-red

dye appears at 1507 cm^{-1} because of the chromophore azo group presence, while a stretching vibration band at 1378 cm^{-1} is typical for the auxochrome sulfonic group.

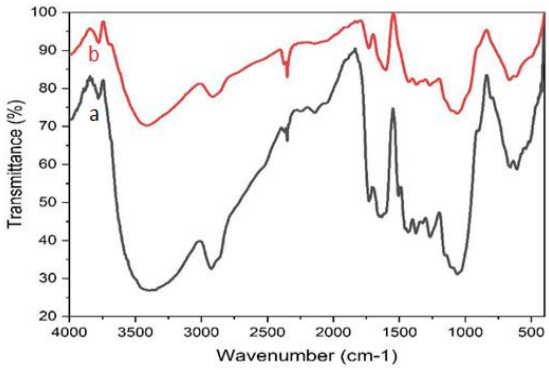

Figure 3:FTIR spectrum of unmodified wood sawdust.

3.1.3. EDX analysis

The sawdust adsorbent's EDX analysis is shown in Figure 4. High percentage of carbon and oxygen is present in the wood sawdust (see Table 1). Functional groups like ethers, aldehydes, ketones, and esters are examples of how oxygen bonds to carbon **[19]**. The EDX plot demonstrated the presence of calcium and copper in trace levels.

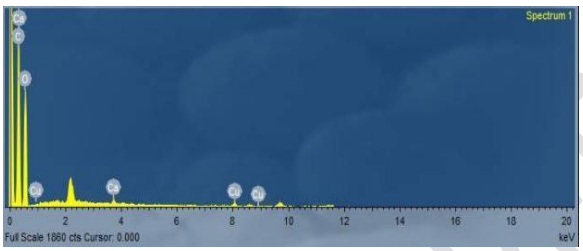

Figure 4:EDX spectrum of unmodified wood sawdust.

Table 1: Chemical composition of unmodified wood sawdust

Element	C	O	Ca	Cu
Weight %	50.79	48.47	0.018	0.56

3.1.4. wood sawdust surface area

The sawdust surface was determined using surface area analyzer. it was calculated on the basis of BET equation. The surface area was found to be 46.15 m^2/g and the average pore size is 3.27 nm.

Brunauer-Emmett-Teller (BET) equation:

$$\frac{P}{V(P^{\circ}-P)} = \frac{1}{V_m C} + \left(\frac{C-1}{V_m C}\right)\frac{P}{P^{\circ}}$$

Where V is the volume of the gas adsorbed at pressure P and temperature T, V_m is the volume of the gas adsorbed to form a saturated monolayer per gram of adsorbent, C is BET constant, and $\frac{P}{P^{\circ}}$is the relative vapor pressure of the gas.

3.1.5 zeta potential distribution

The zeta potential of wood sawdust suspension was found to be −27.2 mV (see Figure 5). At natural pH, the adsorbent net charge is negative. It can be inferred from this that cationic species rather than anionic ones are more likely to be adsorbed using wood sawdust.

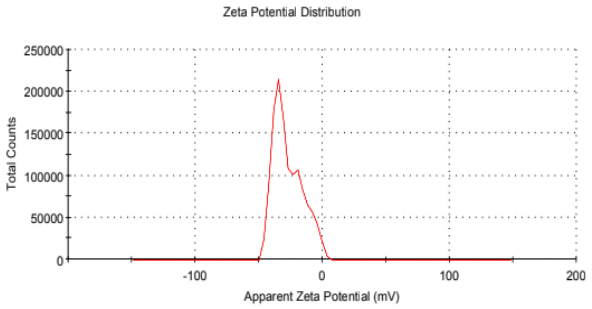

Figure 5: zeta potential distribution of unmodified wood sawdust.

3.2. Application for dye adsorption

The batch approach was used to investigate the adsorptive properties of CR on wood sawdust by controllinga number of experimental factors, including contact time (0–60 min), adsorbent amount (0.1–1.0 g), pH (3–11), starting dye concentration (10–200 mg/l), and adsorption temperature (25–85°C).Except for the ones in which the effects of temperature or pH were examined, all batch experiments were performed in a set of 250 ml Erlenmeyer flasks holding 50 ml of the dye solution at room temperature and pH = 5.

3.2.1. The contact time influence

Figure 6 shows the effect of adsorbent- adsorbate contact time (0- 60 min.) on the removal of CR by SD. The initial dye removal rate was fast due to high driving force, then it gradually decreased as the adsorption proceeded. The curves demonstrate that dye molecules saturate the adsorbent's active sites, and equilibrium is attained **after 10**minutes.

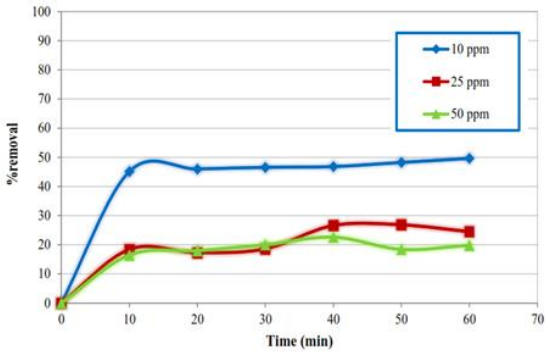

Figure 6: The variation of percentage CR adsorption against the adsorption contact's time. Conditions: 0.1 g adsorbent dosage, natural pH, ambient temperature (25℃) and 240 rpm.

3.2.2. Adsorbent's dosage influence

Figure 7 depicts the effect of varying SD mass from 0.1 to 1.0 g on CR removal efficiency. The adsorption process is greatly influenced by changes in SD mass. As illustrated in Figure 6, the adsorption percentage of CR improves as the adsorbent's dose used increases. This effect is caused by the increase in the material's specific surface area as well as its active sites **[22]**. The optimum dosage was found to be 0.8g, above which the effect of the adsorbent quantity becomes irrelevant due to attaining equilibrium, the percent removal value increases to its highest point with very little fluctuation.

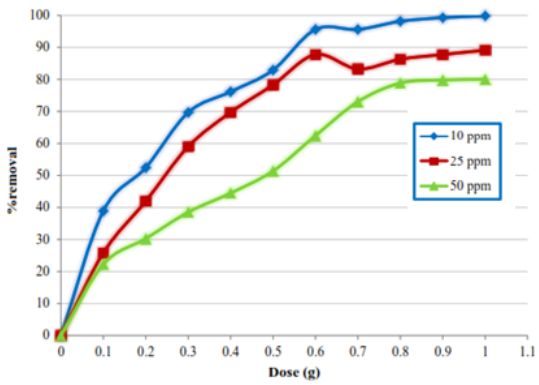

Figure 7: The variation of percentage CR adsorption against the adsorbent dosage. Conditions: 50 min. contact time, ambient temperature (25℃) and 240 rpm.

3.2.3. Initial dye concentration influence

The influence of dye's initial concentration on CR dye adsorption using SD was investigated utilizing experiments performed on solutions with various starting dye concentrations.Figure 8illustrates that as the initial CR concentration increases from 10 to 200 mg/l, the percentage dye removal decreases from 96% to 67%, respectively. This is a result of the high ratio of SD active sites on surface to the initial CR concentration at low CR concentrations. At high dye concentrations, the efficiency of dye removal decreases due to saturation of the adsorbent active sites**[23]**. Theclustering of dye molecules and the subsequent reduction in thermal mobility as a result of the aggregation of adsorbate molecules cause the adsorption rate to decrease **[24]**. Hence, at high concentrations, some CR molecules stay in the solution and are not adsorbed.

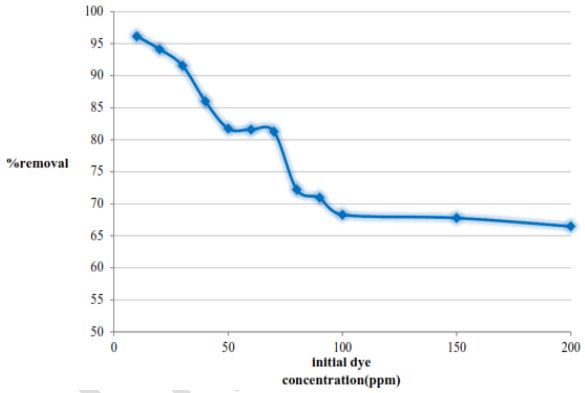

Figure 8: The variation of percentage CR adsorption against the initial dye concentration. Conditions: natural pH, 50 min., ambient temperature (25℃), 0.8 g of adsorbent, and 240 rpm.

3.2.4. Temperature influence

The elimination of Congo red has been investigated at various temperatures in order to determine adsorption isotherms and thermodynamic characteristics. Thermodynamic characteristics that play a significant role in forecasting the adsorption behavior include the heat of adsorption and the energy of activation, both of which are highly temperature-dependent. Increases in temperature have an impact on the adsorbate's solubility, molecular interactions, and chemical potential. The adsorption behavior at different temperatures have been analyzed as shown

in Figure 9.The rate of dye uptake declines with raising temperature from 25-85 °Cdemonstrating that the process is exothermic.This could be as a result of dye molecules' propensity to migrate from the solid phase to the bulk phase when the solution's temperature rises. Raising the temperature can weaken the bonds between the active sites on the adsorbent surface and the adsorbate **[25].**

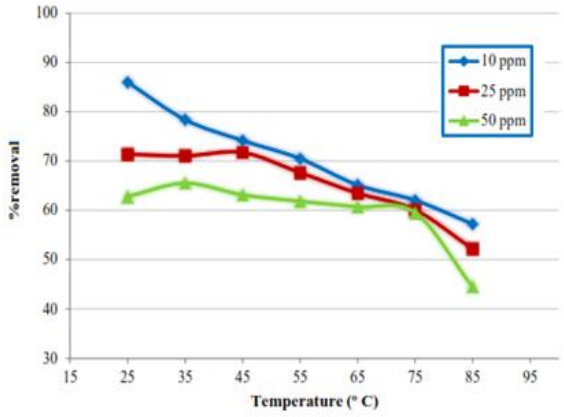

Figure 9: The variation of percentage CR adsorption against the temperature. Conditions: 50 min. contact time, 0.8 g of adsorbent, and 240 rpm.

3.2.5. Solution's pH influence

Thesolution's pH has a significant impact on the adsorptive behavior. The effect of solution pH on CR dye adsorption using SD was investigated through tests carried out at different pHs(2-11). It was found that the dye uptake ascends when the pH is raised from 3 to 5. At highly acidic medium, there are fewer negatively charged surface sites and more positively charged sites, which facilitates the adsorption of dye anions**[22]**. The maximal removal efficiency is achieved at pH=5. Lower adsorption was observed above pH=5 probably because several hydroxyl ions are in competition with CR anions for the same adsorption sites **[23]**(see Figure 10).

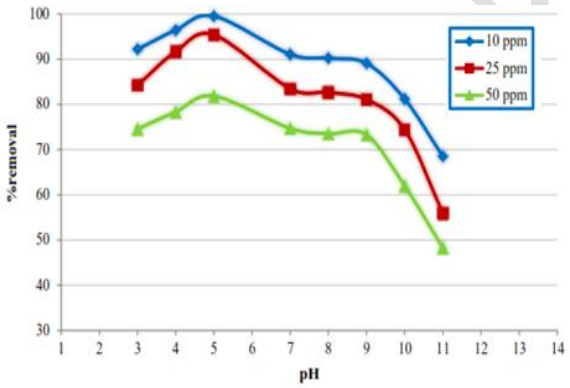

Figure 10: The variation of percentage CR adsorption against pH. Conditions: 50 min. contact time, ambient temperature (25℃), 0.8 g of adsorbent, and 240 rpm.

3.3 Adsorption isotherm investigations

The equilibrium adsorption isotherm is critical for understanding how adsorbate and adsorbent interact and is crucial for adsorption system design.The most popular models used to describe adsorption isotherms are the Temkin, Langmuir, Freundlich, and D-R models (see Figure 11).It was possible to assess the reliability of these models via comparisonof the correlation coefficients (R^2) values of the linear isotherm plots. The results (see Table 2) show

that the Freundlich isotherm model best describes how CR is absorbed by wood sawdust ($R^2 = 0.9771$). Table 3 compares SD's maximal adsorption capacity to that of other adsorbents described in the literature for the removal of CR. According to that comparison, unmodified wood has a good adsorption capacity for CR.

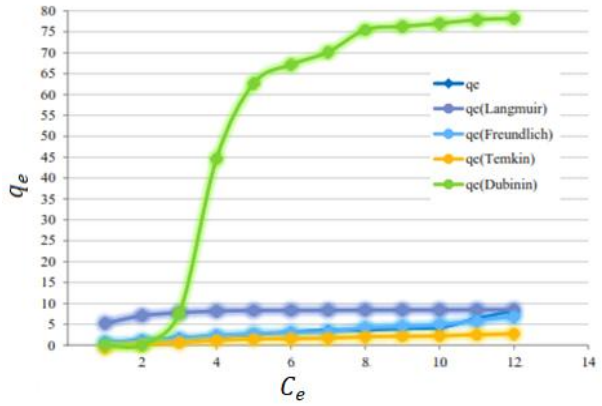

Figure 11: C_e vs. q_e for experimental data and the different isotherm models.

Table 2. Isotherms constants and regression data for various adsorption isotherms for adsorption of CR by SD.

Isotherms	Linear expression	parameters	correlation coefficients
Langmuir	$\frac{c_e}{q_e} = \frac{1}{q_m k_l} + \frac{c_e}{q_m}$	$q_m = 8.510638\ mg/g$ $k_l = 4.194292\ l/mg$	0.8115
Freundlich	$\ln q_e = \frac{1}{n} \ln c_e + \ln k_f$	$k_f = 0.9997\ l/mg$ $n = 2.176752$	0.9771
Temkin	$q_e = q_m \ln k_t + q_m \ln c_e$	$q_m = 0.6305\ mg/g$ $k_t = 11.419496\ l/mg$	0.7801
D- R	$\ln q_e = \ln q_m - D\varepsilon^2$	$q_m = 78.57864733\ mg/g$ $D = 3.4123\ mol^2/kJ^2$	0.6052

Table 3. Comparison between the maximum capacity of various solid desiccant used for Congo-red adsorption.

Solid desiccant	Maximum capacity, mg/g	Reference
Biochar from residual algae	51.3	[26]
Cellulose acetate/chitosan/ SWCNT/Fe_3O_4/TiO_2 composite nanofibers	74.2	[27]
Magnetic peanut husk	56.3–79	[28]
Fly-ash@Fe_3O_4	153	[29]
Mycelial pellet	316.4	[30]

bentonite	20.56	[31]
Activated pine cone	40.2	[32]
Clinoptilolite	16.92	[33]
Fe_3O_4/NiO nanocomposite	210.78	[34]
Unmodified wood sawdust	8.55	Present study

3.4 Adsorption kinetics

Pseudo-first-order and second-order kinetic models were tested with the experimental data utilizing graphical representations of the linear equations in order to comprehend the kinetics of CR removal using SD as an adsorbent. Table 4 contains a list of the two kinetic models' parameters. The correlation coefficient firmly establishes the pseudo-second-order kinetic model's compliance with the adsorption of CR utilizing SD ($R^2 = 0.9982$), in which chemisorption is the rate limiting step.

Table 4. Pseudo-first-order and second order kinetic model's parameters for the adsorption of CR usingSD.

Adsorption kinetic model	parameters	correlation coefficients
pseudo-first-order	$k_1 = 0.164665$	0.51840
pseudo-second-order	$k_2 = 0.398712$	0.99820

3.5 Thermodynamics parameters

They are calculated according to Van't Hoff equation as follows:

$$K = \frac{q_e}{c_e}$$

$$\ln K = \frac{\Delta S}{R} - \frac{\Delta H}{RT}$$

$$\Delta G = -RT \ln K$$

Where: R is the gas constant (8.314 J /mol. K) and T is the temperature in kelvin.

The intercept and slope of Figure 12 were used to determine both the enthalpy change (ΔH) and the entropy change (ΔS) (see Table 5). The spontaneous character of adsorption, along with sawdust's strong affinity for Congo red, are both confirmed by the negative values of ΔG. The fact that the negative value of ΔG° decreases as temperature rises suggests that lower temperatures are more suitable for the adsorption of CR via SD**[16]**.

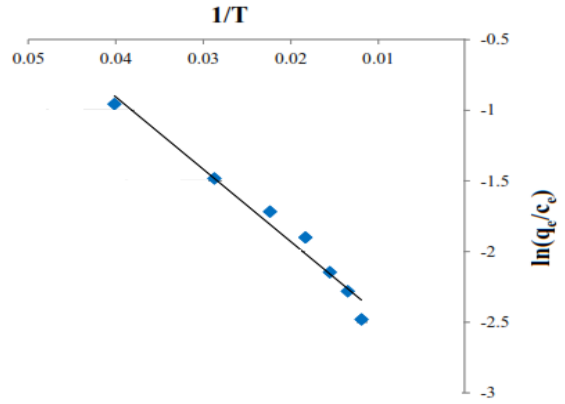

Figure 12: Graphical determination of ΔH and ΔS.

Table 5 Values of thermodynamic parameters for the adsorption of CR by using wood sawdust.

Temperature (K)	$\Delta G\ (kJ.mol^{-1})$	$\Delta H\ (kJ.mol^{-1})$	$\Delta S\ (kJ.mol^{-1}K^{-1})$
298.15	6877.335354	-426.00936	-24.4955382
308.15	7122.290736		
318.15	7367.246118		
328.15	7612.2015		
338.15	7857.156882		
348.15	8102.112264		
	8347.067646		

3.6 Designofbatch adsorber

According to the experimental equilibrium data, the batch adsorber's design is determined. The sorption system's mass balance equation has the form [1],

$$V(C_i - C_e) = M(q_e - q_i) \qquad (13)$$

where$C_i$and $C_e$are the starting and equilibrium dye concentration(mg/l),respectively.The solid phase starting and equilibrium concentrations, expressed in mg/g, are denoted by the symbols $q_i$and q_e, respectively. Since the adsorption equilibriumdata best fits Freundlich model, it was utilized for $q_e$calculation.The design equation is [1],

$$\frac{M}{V} = \frac{(C_i - C_e)}{q_e} \qquad (14)$$

Figure 13(a) represents thechange ofadsorbentdosevs. effluent volumeat initial dye concentration 10 mg/l and percentage removal range from 10-90%. while, Figure 13(b) representsthe change of adsorbentdosevs.effluent volumeat 90% removalandarange ofsolutionconcentrationfrom10to100mg/l.

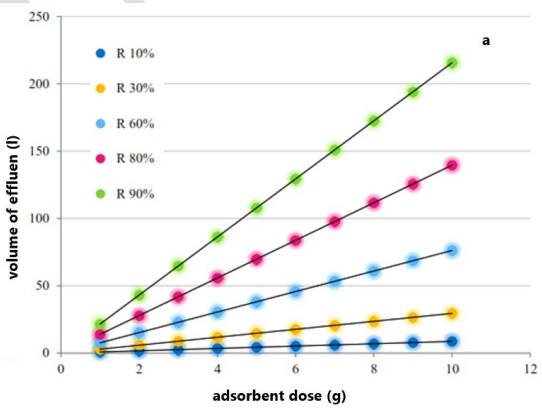

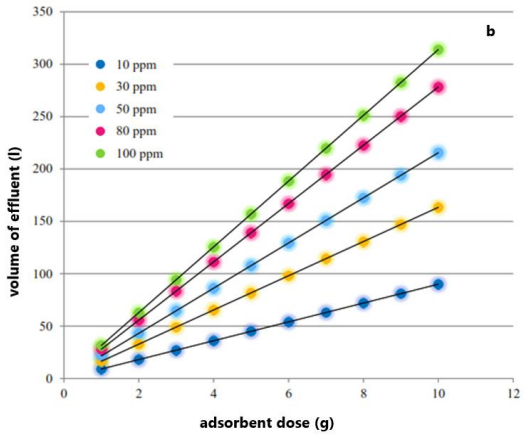

Figure 13. Volume of effluent treated versus adsorbent dose. (a) at different percentage removal of 10 mg/l CR concentration, (b) at 90% removal at different initial CR concentrations.

4. Conclusions

It was feasible to successfully conduct batch adsorption of the azo dye Congo red (CR) on extremely cheap wood sawdust that had not been treated. This was a successful process. Research was carried out in order to ascertain the manner in which the sorption process is influenced by a variety of distinct elements. These factors include the length of contact, the amount of solid adsorbent, the initial concentration of adsorbate, temperature, and pH. Following a period of ten minutes at a temperature of 25 degrees Celsius and a pH of 5, the removal efficiency reached its greatest point. For the purpose of determining the properties of the adsorbent, experiments using FTIR, SEM, EDX, and BET were carried out. The equilibrium isotherms were characterized by using four distinct models. These models were employed in order to establish equilibrium. After analyzing the data, it was discovered that the Freundlich model offered the most accurate representation of the data (R^2 = 0.9771). A pseudo-second-order model is the most accurate depiction of the process, according to the findings of the kinetic research (R^2 = 0.9982), which found that the model was the most accurate. During the course of the thermodynamic investigation, the spontaneous and exothermic nature of the sorption process was brought to light. The optimal isotherm model, which served as the foundation for the design, was used in the process of developing a one-stage batch adsorber for the purpose of sorption of CR onto wood sawdust.

6. References

1. R. A. Mansour, Riham Atef, R. R. Elazaby& A. A. Zaatout. Experimental study on the adsorption of Cr^{+6} and Ni^{+2} from aqueous solution using low-cost natural material.International journal of phytoremediation, 22(5): 508–517, (2020). http://dx.doi.org/10.1080/15226514.2019.1683716

2. Riham Atef, N. M. Aboeleneen, and Nabil M. AbdelMonem. Preparationand characterization of low-cost nano-particle material using pomegranate peels for brilliant green removal.International journal of phytoremediation. 25(1), (2023).
https://doi.org/10.1080/15226514.2022.2056133

3. O.G. Allam, N.A. Fathy , M. G. Khafagj and M.K. El-Bisi. Modified waste materials for removal of cationic dye from liquid Effluents and their kinetic studies, Egypt J. Chem. 58 (2):141-154, (2015).
https://doi.org/10.21608/EJCHEM.2015.979

4. Sarah Elhady, M. Bassyouni, R. A. Mansour, Medhat H. Elzahar, Mamdouh Y. Saleh. Developed Method for Treatment of Industrial Wastewater from Edible Oil Industry using Membrane Technology. International Journal of Engineering and Advanced Technology, 9(3), (2020). https://doi.org/10.35940/ijeat.C5940.029320
5. Mahmoud A. Abdelaziz , Medhat E. Owda , Ragab E. Abouzeid , Omaymah Alaysuy , ELsiddig Idriss Mohamed. Kinetics, isotherms, and mechanism of removing cationic and anionic dyes from aqueous solutions using chitosan/magnetite/silver nanoparticles https://doi.org/10.1016/j.ijbiomac.2022.11.203
6. Said Benkhaya,a, Souad M'rabet,b, and Ahmed El Harfia. Classifications, properties, recent synthesis and applications of azo dyes.Heliyon, 6(1), e03271, (2020).https://doi.org/10.1016/j.heliyon.2020.e03271
7. Araceli Verônica F. N. Ribeiro, André Romero da Silva, Madson de Godói Pereira, Marcus Vinicius Vaughan Jennings Licinio, Joselito Nardy Ribeiro. Wood Sawdust Powder from Corymbia Citriodora to Congo Red Toxic Dye Adsorption. Indian Journal of Applied Research, 8 (7), (2018). PRINT ISSN No 2249-555X https://doi.org/10.36106/IJAR
8. M.K. Purkait , A. Maiti , S. DasGupta , S. De. Removal of Congo red using activated carbon and its regeneration. Journal of Hazardous Materials 145: 287–295, (2007). https://doi.org/10.1016/j.jhazmat.2006.11.021
9. Venkat S. Mane, P.V. Vijay Babu. Kinetic and equilibrium studies on the removal of Congo red from aqueous solution using Eucalyptus wood (Eucalyptus globulus) saw dust.Journal of the Taiwan Institute of Chemical Engineers 44: 81–88,(2013). https://doi.org/10.1016/j.jtice.2012.09.013
10. Sarah Goudjil, Saadia Guergazi, Toufik Masmoudi, Samia Achour. Effect of reactional parameters on the elimination of Congo Red by the combination of coagulation–flocculation with aluminum sulfate. Desalination and Water Treatment 209: 429–436, (2021). https://doi.org/10.5004/dwt.2021.26474
11. Yunhan Jia, Lei Ding, Peiyue Ren, Meiying Zhong, Jiangya Ma, and Xiaoran Fan, Performances and Mechanism of Methyl Orange and Congo Red Adsorbed on the Magnetic Ion-Exchange Resin. J. Chem. Eng. Data, 65(2): 725–736, (2020). https://doi.org/10.1021/acs.jced.9b00951
12. Nisar Ali, Amir Said, Farman Ali, Fazal Raziq,Zarshad Ali, Muhammad Bilal, Laurence Reinert,Tasleem Begum & Hafiz M. N. Iqbal. Photocatalytic Degradation of Congo Red Dye from Aqueous Environment Using Cobalt Ferrite Nanostructures: Development, Characterization, and Photocatalytic Performance. Water Air Soil Pollut., 231: 50, (2020). https://doi.org/10.1007/s11270-020-4410-8
13. Ghada M. Mohamed, Ola I. El-Shafey, Nady A. Fathy. Preparation of carbonaceous hydrochar adsorbents from cellulose and lignin derived from rice straw, Egypt. J. Chem. 60 (5):793 –804, (2017). https://doi.org/10.21608/ejchem.2017.1311.1080
14. Mohammad Shafiqul Alam, Rexona Khanom, Mohammad Arifur Rahman. Removal of Congo Red Dye from Industrial Wastewater byUntreated Sawdust. American Journal of Environmental Protection. 4(5): 207-213, (2015). https://doi.org/10.11648/j.ajep.20150405.12
15. Mohebali, S., Bastani, D., Shayesteh, H. Methylene blue removal using modified celery (Apium graveolens) as a low-cost biosorbent in batch mode: Kinetic, equilibrium, and thermodynamic studies. J. Mol. Struct. 1173: 541–551, (2018). https://doi.org/10.1016/j.molstruc.2018.07.016
16. Shayesteh,H., Nodehi, R., Rahbar-Kelishami, A.Trimethylamine functionalized clay for highly efficient removal of diclofenac from contaminated water: Experiments and theoretical calculations. Surf. Interfaces 20, 100615, (2020). https://doi.org/10.1016/j.surfin.2020.100615

17. Shayesteh, H., Raji, F., Kelishami, A.R. Influence of the alkyl chain length of surfactant on adsorption process: A case study. Surf. Interfaces 22, 100806, (2021). https://doi.org/10.1016/j.surfin.2020.100806

18. Sushmita Banerjee, M.C. Chattopadhyaya, Adsorption characteristics for the removal of a toxic dye, tartrazine from aqueous solutions by a lowcost agricultural by-product. Arabian Journal of Chemistry, 10(2): S1629-S1638, (2017). https://doi.org/10.1016/j.arabjc.2013.06.005

19. Najeeb ur Rahman, Ihsan Ullah , Sultan Alam , Muhammad Sufaid Khan , Luqman Ali Shah , Ivar Zekker, Juris Burlakovs , Anna Kallistova,NikolaiPimenov,Zane Vincevica-Gaile,YahyaJani and Mohammad Zahoor. Activated Ailanthus altissima Sawdust as Adsorbent for Removal of Acid Yellow 29 from Wastewater: Kinetics Approach. Water, 13(15), 2136, (2021). https://doi.org/10.3390/w13152136

20. Congjin Chen, Jianju Luo, Wen Qin, Zhangfa Tong. Elemental analysis, chemical composition, cellulose crystallinity, and FT-IR spectra of Toona sinensis wood.Monatsh Chem, 145:175–185, (2014). https://doi.org/10.1007/s00706-013-1077-5

21. F Hemmati, SM Jafari, RA Taheri. Optimization of homogenization-sonication technique for the production of cellulose nanocrystals from cotton linter. Internationaljournal of biological macromolecules, 137:374-381, (2019). https://doi.org/10.1016/j.ijbiomac.2019.06.241

22. Peyman Koohi, Ahmad Rahbar-kelishami, Hadi Shayesteh. Efficient removal of Congo red dye using Fe_3O_4/NiO nanocomposite: Synthesis and characterization. Environmental Technology and Innovation, 23, 101559, (2021). https://doi.org/10.1016/j.eti.2021.101559

23. Kangli Wu, Xiaomei Pan, Jianqiang Zhang, Xiaomeng Zhang, Abdramane Salah zene, and Yongqiang Tian. Biosorption of Congo Red from Aqueous Solutions Based on SelfImmobilized Mycelial Pellets: Kinetics, Isotherms, and Thermodynamic Studies. ACS Omega, 5: 24601−24612, (2020). https://doi.org/10.1021/acsomega.0c03114

24. Barsharani Priyadarshini, Tanaswini Patra, Tapas Ranjan Sahoo. An efficient and comparative adsorption of Congo red and Trypan blue dyes on MgO nanoparticles: Kinetics, thermodynamics and isotherm studies. Journal of Magnesium and Alloys, 9(2): 478-488, (2021). https://doi.org/10.1016/j.jma.2020.09.004

25. Khaoula Litefti, M. Sonia Freire, Mostafa Stitou, and JuliaGonzález-Álvarez. Adsorption of an anionic dye (Congo red) from aqueous solutions by pine bark. ScientificReports, 9, Article number: 16530, (2019). https://doi.org/10.1038/s41598-019-53046-z

26. Nautiyal, P., Subramanian, K. A., Dastidar, M. G. Adsorptive removal of dye using biochar derived from residual algae after in-situ transesterification: Alternate use of waste of biodiesel industry. J. Environ. Manage. 182: 187−197, (2016). https://doi.org/10.1016/j.jenvman.2016.07.063

27. Zabihi Sahebi, A., Koushkbaghi, S., Pishnamazi, M., Askari, A. Khosravi, R., Irani, M. Synthesis of cellulose acetate/chitosan/SWCNT/Fe_3O_4/TiO_2 composite nanofibers for the removal of Cr(VI), As(V), Methylene blue and Congo red from aqueous solutions. Int. J. Biol. Macromol. 140: 1296–1304, (2019). https://doi.org/10.1016/j.ijbiomac.2019.08.214

28. Aryee, A.A., Dovi, E., Han, R., Li, Z., Qu, L. One novel composite based on functionalized magnetic peanut husk as adsorbent for efficient sequestration of phosphate and Congo red from solution: Characterization, equilibrium, kinetic and mechanism studies. J. Colloid Interface Sci. 598: 69–82, (2021). https://doi.org/10.1016/j.jcis.2021.03.157

29. Maria Harja, Nicoleta Lupu, Horia Chiriac, Dumitru-Daniel Herea and Gabriela Buema. Studies on the Removal of Congo Red Dye by an Adsorbent Based on Fly-Ash@Fe3O4 Mixture. Magnetochemistry. 8: 125, (2022). https://doi.org/10.3390/magnetochemistry8100125

30. Kangli Wu, Xiaomei Pan, Jianqiang Zhang, Xiaomeng Zhang, Abdramane Salah zene, and Yongqiang Tian. Biosorption of Congo Red from Aqueous Solutions Based on Self-Immobilized Mycelial Pellets: Kinetics, Isotherms, and Thermodynamic Studies. ACS Omega. 5: 24601−24612, (2020) https://doi.org/10.1021/acsomega.0c03114

31. Taher, T., Mohadi, R., Rohendi, D., Lesbani, A. Kinetic and thermodynamic adsorption studies of Congo red on bentonite. In: AIP Conference Proceedings. American Institute of Physics Inc. (2017). http://doi.org/10.1063/1.4978101.

32. Dawood, S., Sen, T.K. Removal of anionic dye Congo red from aqueous solution by raw pine and acid-treated pine cone powder as adsorbent: Equilibrium, thermodynamic, kinetics, mechanism and process design. Water Res. 46: 1933–1946, (2012). http://dx.doi.org/10.1016/j.watres.2012.01.009

33. Nodehi, R., Shayesteh, H., Kelishami, A.R., 2020. Enhanced adsorption of Congo red using cationic surfactant functionalized zeolite particles. Microchem. J. 153:104281, (2020). http://doi.org/10.1016/j.microc.2019.104281.

34. Peyman Koohi, Ahmad Rahbar-kelishami, Hadi Shayesteh. Efficient removal of Congo red dye using Fe_3O_4/NiO nanocomposite: Synthesis and characterization. Environmental Technology & Innovation 23: 101559, (2021). http:// doi.org/10.1016/j.eti.2021.101559